ARTICLES
PUBLISHED ONLINE: 3 JUNE 2012 | DOI: 10.1038/NCHEM.1367
nature chemistry

An ultrasensitive universal detector based on neutralizer displacement

Jagotamoy Das[1], Kristin B. Cederquist[1], Alexandre A. Zaragoza[1], Paul E. Lee[1], Edward H. Sargent[2] and Shana O. Kelley[1,3]*

Diagnostic technologies that can provide the simultaneous detection of nucleic acids for gene expression, proteins for host response and small molecules for profiling the human metabolome will have a significant advantage in providing comprehensive patient monitoring. Molecular sensors that report changes in the electrostatics of a sensor's surface on analyte binding have shown unprecedented sensitivity in the detection of charged biomolecules, but do not lend themselves to the detection of small molecules, which do not carry significant charge. Here, we introduce the neutralizer displacement assay that allows charge-based sensing to be applied to any class of molecule irrespective of the analyte charge. The neutralizer displacement assay starts with an aptamer probe bound to a neutralizer. When analyte binding occurs the neutralizer is displaced, which results in a dramatic change in the surface charge for all types of analytes. We have tested the sensitivity, speed and specificity of this system in the detection of a panel of molecules: (deoxy)ribonucleic acid, ribonucleic acid, cocaine, adenosine triphosphate and thrombin.

The development of universal sensors that can detect a broad range of different molecular targets is highly desirable, as such versatile platforms offer a single solution for tests that have traditionally required the use of a number of different types of instrumentation. To date, very few universal detection systems have been developed[1,2], and none has shown sufficient sensitivity for direct sample analysis or clinical use. The development of detection methods that are rapid and more sensitive than those currently available will fulfil unmet needs in screening for drugs of abuse, medical diagnosis, point-of-care testing and environmental monitoring.

Sensing approaches that report on changes in the electrostatics of a sensor-immobilized monolayer have been developed with a variety of readout strategies, including field-effect transistors (FETs), microcantilevers and electrochemical sensors[3–11]; however, an effective method that can sensitively detect nucleic acid, protein and small molecule analytes has remained elusive. Electrochemical signalling methods have attracted particular attention for fast, sensitive, portable and cost-effective detection[12–31]. Switch-based electrochemical biosensors show exceptional promise for versatile detection[22], but with limited sensitivity towards nucleic acid analytes that therefore requires enzymatic amplification of the target sequences[23].

Here we use a new approach to electrochemical detection, the neutralizer displacement assay (NDA), which achieves record-breaking sensitivity with all of the major classes of biologically relevant molecules. The principle that underlies the NDA is illustrated in Fig. 1. In traditional assays (Fig. 1a), a probe molecule is tethered to the surface of an electrode. Thus, prior to analyte introduction, the charge of the sensor is determined by this probe molecule. After binding by the analyte, the state of charge is changed by the charge of the analyte, which leads to three limitations in traditional charge-based sensing methods. First, the background signal may be large, although using neutral probes such as peptide nucleic acid (PNA) can overcome this first limitation. Second, the ratio of signal:background may be small if the charge of the probe dominates the charge of the analyte. Third, the sign of the signal is determined by the analyte, which often leads to a 'signal-off' assay structure that can produce a high false-positive rate. In sum, traditional methods of sensing are, because of their signal amplitude, their signal-to-background ratio and their sign of signal change, at the mercy of the analyte. However, the choice of analyte is not a degree of freedom available to the assay designer to explore, but rather is a requirement of the test.

The NDA (Fig. 1b) introduces a new freedom in the design of the electrostatic character of the sensor surface. A probe molecule is tethered to the surface of an electrode and is joined by a neutralizer, which is a conjugate of PNA and cationic amino acids that specifically binds to the probe and neutralizes the charge of the probe. The probe–neutralizer complex is designed to include mismatches such that the analyte of interest binds the probe more strongly, rapidly and robustly, which leads to displacement of the neutralizer. With the NDA, all three limitations of traditional charge-sensing assays are overcome. The background signal is now suppressed strongly through engineered charge compensation. The signal changes that correspond to the presence of an analyte are determined not only by the molecular charge of the molecule, but also by the charge of the probe molecule that is unmasked on binding. Finally, the sign and amplitude of the signal is determined not only by the charge of the analyte, but also by that of the probe.

To test the NDA concept, we used an electrocatalytic reporter system that provides a signal proportional to the charge change at electrode surfaces[24]. This system was previously used with nanostructured microelectrodes (NMEs)[25–31] that can be fabricated on the surface of a chip, and both proteins and nucleic acids could be detected with high levels of sensitivity. Prior to the development of the NDA concept, the NME electrochemical platform, like its counterparts in FET and nanowire-based direct electronic sensing, failed to offer the capacity to detect small molecules.

Results and discussion

Sensor fabrication. Using photolithographic patterning, we produced an array of sensors on the surface of a microelectronic

[1]Department of Pharmaceutical Sciences, Leslie Dan Faculty of Pharmacy, University of Toronto, Toronto, Canada, [2]Department of Electrical and Computer Engineering, Faculty of Engineering, University of Toronto, Toronto, Canada, [3]Department of Biochemistry, Faculty of Medicine, University of Toronto, Toronto, Canada. *e-mail: shana.kelley@utoronto.ca

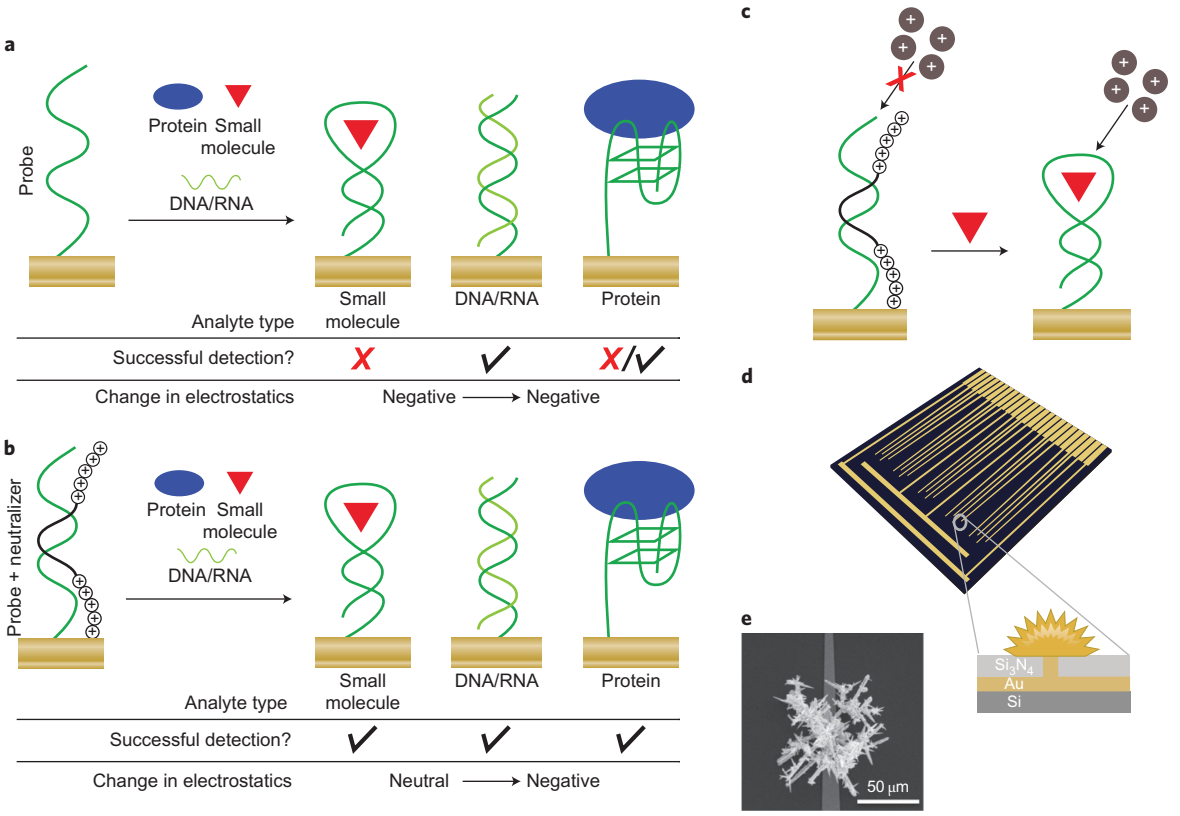

Figure 1 | Summary of the NDA and sensor chips utilized for testing. a, In traditional electrostatic detection without NDA only large changes in the electrostatic profile are detectable, for example DNA/DNA binding or the binding of a highly charged protein. **b**, In NDA detection, small molecules, nucleic acids and proteins are all detectable as each one causes displacement of a neutralizer and a large change in charge. **c**, The neutralizer–probe complex attenuates reporter-ion binding. The release of the neutralizer on the addition of the target changes the electrostatics to negative, which yields an increased electrocatalytic current. **d**,**e**, Schematic (**d**) of a sensor chip that possesses 20 nanostructured electrodes with structures as shown in (**e**).

chip (Fig. 1d). The chips used in this study possessed 20 sensors. With the use of a SiO_2-coated silicon wafer as a base, contact pads and leads were patterned onto individual chips. A layer of Si_3N_4 was then used to passivate the surface of the chip. To provide a template for the growth of electrodeposited sensors, photolithography was used next to open 5 μm apertures in the Si_3N_4. Subsequently, Au electrodeposition was employed to grow fractal microstructures, the size and morphology of which can be modulated by deposition time, potential, Au concentration, supporting electrolyte and overcoating protocol[25,30]. As nanostructures increase the sensitivity of the assay significantly, we coated the Au structures with a thin layer of Pd to form finely nanostructured sensors (Fig. 1e)[30]. The sensors generated were characterized using electrochemical methods, as shown in Supplementary Fig. S11 and as previously described[25,27,30].

Detection of adenosine triphosphate (ATP). To examine the ability of our neutralizer assay to detect small molecules, we chose ATP as a model molecule. ATP is a well-known cellular energy source and is involved in driving a number of biological processes. The configuration of the neutralizer assay for ATP detection is shown in Fig. 2a. Thiolated ATP-binding aptamers were first immobilized onto sensors with Pd on their surface, after which a partially complementary neutralizer was introduced. The PNA portion of the neutralizer is primarily complementary to the aptamer; however, we introduced two mismatches for facile liberation of the neutralizer on ATP addition (Table 1, underlined portions). The presence of the neutralizer, because of the appended lysine residues, strongly reduces the charge at the sensor surface, which can be restored by the displacement of the neutralizer by a target molecule. In studies of the optimal neutralizer structure (Supplementary Fig. S6), it was determined that the structure used here, with five lysines at each end, was optimal for the maximal background suppression and displacement in the presence of analyte.

To measure the change of charge at the sensor surface, we used a previously developed $[Ru(NH_3)_6]^{3+}/[Fe(CN)_6]^{3-}$ catalytic reporter system to generate a signal that can be monitored by differential pulse voltammetry (DPV) (Fig. 1)[24]. In this system, the primary electron acceptor $[Ru(NH_3)_6]^{3+}$ is attracted electrostatically to the electrode surface in proportion to the amount of phosphate-bearing nucleic acid. When $[Fe(CN)_6]^{3-}$ is used during the electrochemical readout, Ru(III) is regenerated chemically by $[Fe(CN)_6]^{3-}$ to form a redox cycle, which amplifies the signal significantly[24]. This method is free of covalent labels and does not require preprocessing of the samples. High catalytic currents are expected when only DNA aptamer probes are immobilized on the sensors because of the electrostatic affinity of Ru(III) for the phosphate groups of the DNA backbone, but these currents would be attenuated strongly in the presence of the neutralizer.

Figure 2b shows DPV signals obtained at the sensors before addition of the neutralizer, after addition of the neutralizer and after target introduction. Scans of immobilized aptamers revealed a high catalytic current, consistent with the strong electrostatic attraction of Ru(III) to the DNA backbone. The current (I) is reduced by >80% when the neutralizer molecule is hybridized to the aptamer. When ATP (1 mM) binds to the aptamer probe, a structural change of the aptamer causes a release of the neutralizer, which leads to an increase in catalytic current (Fig. 2b). The change

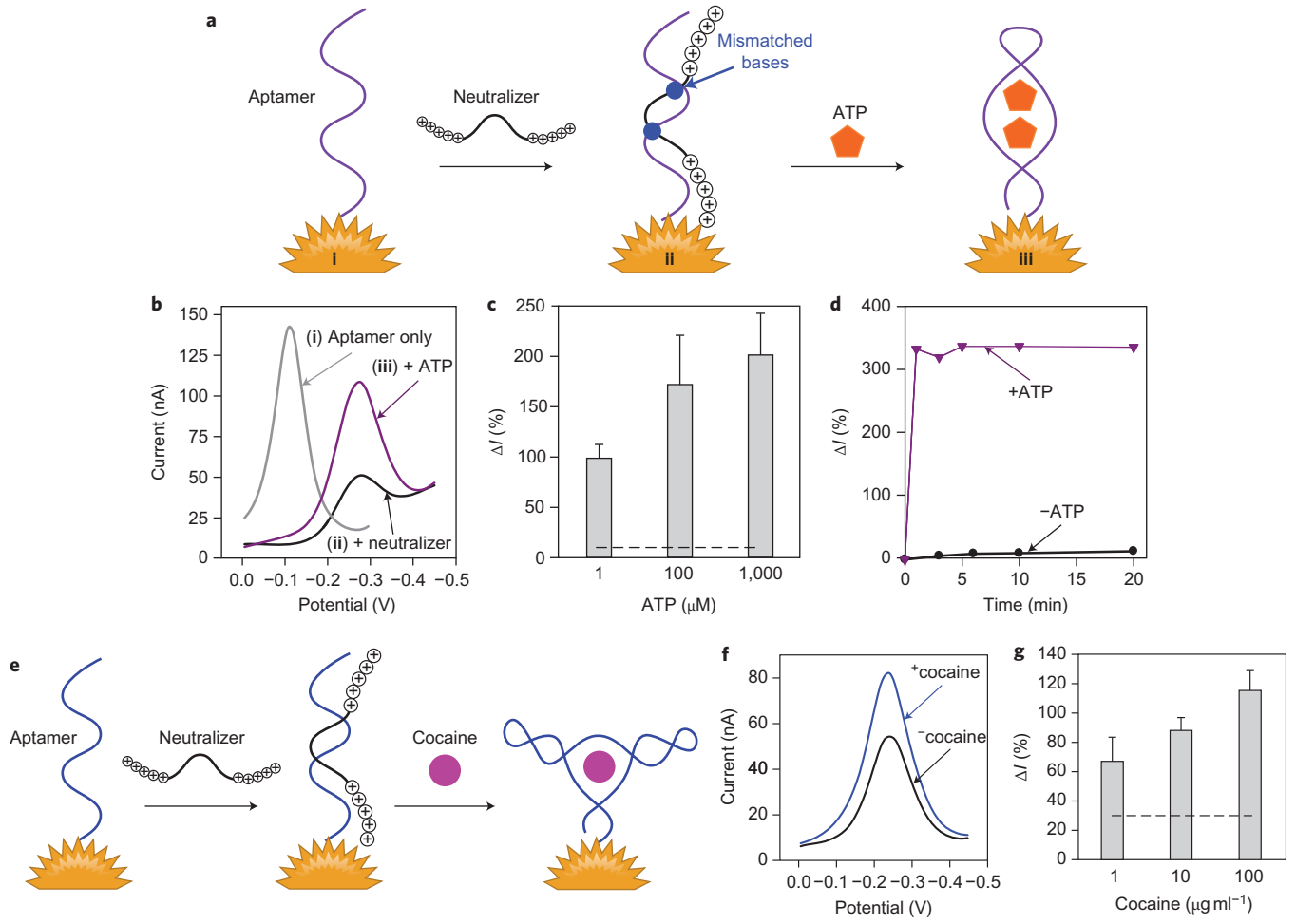

Figure 2 | NDA small molecule detection: ATP and cocaine. a, Schematic representation of ATP detection by NDA. **b**, DPVs for ATP-binding aptamer-modified NME (**i**), after neutralizer binding to the aptamer (**ii**) and after treatment with 1 mM ATP (**iii**). **c**, Concentration-dependent signal changes for ATP detection. The horizontal dashed line indicates the average signal change in the absence of ATP or a non-cognate analyte. **d**, Time-dependent signal change for the addition of 100 μM (purple line) and 0 μM (black line) ATP. **e**, Schematic representation of the cocaine-detection assay. **f**, DPV signals before (black line) and after (blue line) the addition of 1 μg ml^{-1} of cocaine. **g**, Concentration-dependent data for cocaine detection. The horizontal dashed line indicates the average signal change in the absence of cocaine. Non-cognate analytes produced similar background levels. Error bars represent the standard error and are collected from at least three independent experiments on three chips that have 20 sensors. Averaged data from single chips exhibit significantly lower error values (<20%).

of current (ΔI%) from before ATP binding to after ATP binding directly reflects how much ATP is present in the solution (Fig. 2c).

The Ru^{3+} reduction peak shifts to more negative potentials for the neutralized versus non-neutralized probe, probably because the kinetics of electron transfer are slowed when the neutralizer is present, given that the Ru^{3+} is no longer surface bound[32]. We observed that the reduction peak does not shift back all the way on analyte binding. As there is a shift even when the sensor is not neutralized completely (Supplementary Fig. S5), we can explain the incomplete shift back through a picture in which the neutralizer is not displaced quantitatively for the concentrations of analyte described herein. Detailed studies are underway to characterize the redox properties of the reporter groups used here as a function of surface neutralization and the structure of the neutralizer used and will be reported on elsewhere.

To evaluate the time dependence of the sensor response, we introduced ATP into the $[Ru(NH_3)_6]^{3+}/[Fe(CN)_6]^{3-}$ catalytic solution and measured signal changes in real time. The data shown in Fig. 2d indicate that signal changes in the presence of ATP occur within one minute, and the signal change in the absence of ATP is not significant even after 20 minutes. These results clearly indicate that sensor response is rapid and that the probe–neutralizer complex is stable.

Detection of cocaine. After observing that our chip-based neutralizer assay was effective for ATP detection, we attempted to use it in the detection of cocaine. Rapid screening methods for this drug of abuse are an urgent and unmet need. The assay was carried out using the same strategy as described above for ATP, with a cocaine-specific aptamer as the receptor (Fig. 2e). As observed for ATP, the initial high current of the cocaine-binding aptamer decreased after neutralizer hybridization. When the aptamer–neutralizer complex was challenged with cocaine, the resulting structural change of the aptamer released the neutralizer and resulted in a high catalytic current (Fig. 2f). The signal change for 1 μg ml^{-1} cocaine was >60% higher than that in the absence of cocaine or in the presence of a non-target analyte. This level of sensitivity is comparable with commercial tests and is ample for drug screening. Figure 2g shows the concentration dependence of the signal change observed with the addition of cocaine. The dynamic range of the assay is somewhat narrow, but could be improved if sensor morphology was tuned as previously described[25].

Table 1 | Sequences used in this work.

Name	Type	Sequence*,†
ATP-binding aptamer	DNA	ACC TGG GGG AGT ATT GCG GAG GAA GGT TTT-C_3-SH
ATP aptamer neutralizer	PNA	KKKKK-TCC ACA ATA CCC CCC-KKKKK
Cocaine-binding aptamer	DNA	HS-C_6-GAC AAG GAA AAT CCT TCA ATG AAG TGG GTC
Cocaine aptamer neutralizer	PNA	KKKKK-CAT AGA AGA ATT TTC-KKKKK
Thrombin-binding aptamer	DNA	HS-C_6-GGT TGG TGT GGT TGG
Thrombin aptamer neutralizer	PNA	KKKKK-CGA CAG CAA-KKKKK
Probe for *E. coli* lysate/total RNA/20-mer target	DNA	HS-C_6-ATC TGC TCT GTG GTG TAG TT
Neutralizer for DNA probe	PNA	KKKKK-CTA CAC CCC AAA GCA G-KKKKK
20-mer target	DNA	AAC TAC ACC ACA GAG CAG AT
20-mer non-complementary target	DNA	ATT GCA TCA ATG TCT TAC TT

*5′ to 3′ for DNA sequences, N to C terminus for PNA sequences. †Underlined portions denote single-base mismatches in neutralizers.

Detection of DNA. With a high level of performance established for small molecule analytes, we investigated whether this assay could also exhibit clinically relevant (fM or better) sensitivity against nucleic acid analytes, as other attempts to develop universal detection systems have not been successful in achieving good sensitivity with this analyte class.

Figure 3a is a schematic representation of the neutralizer assay applied towards nucleic acid targets. A thiolated-DNA probe was immobilized on the NMEs and, as expected, initially the catalytic current for the DNA probe was high (Fig. 3b) and significantly suppressed on addition of the neutralizer. Smaller NMEs were used in these trials to allow a comparison of the limits of detection of NDA with prior studies[25]. After treatment with a 1 pM complementary oligonucleotide target, the current increased by >300%. The specific binding of the neutralizer to the probe was also confirmed using gel electrophoresis (see Supplementary Fig. S1).

Next, we investigated the concentration dependence of the nucleic acid NDA with a 20-mer synthetic target DNA. A non-complementary target was used to evaluate both background levels and specificity. To identify the detection limit of our assay, we titrated the concentration of target DNA down to 10 aM (Fig. 3c). The ΔI% increased with increasing concentration of the target within a range that spanned five orders of magnitude. The horizontal dashed line indicates the average currents observed with a 100 nM non-complementary target. The signal change for 10 aM of DNA target, although above that of the 100 nM non-complementary target, was not high enough to be statistically significant, which indicates that the detection limit of our assay for the 20-mer target is ~100 aM.

The suitability of the assay to analyse samples that are more heterogeneous was assessed by analysing DNA detection in undiluted human serum (Supplementary Fig. S7). Comparison of the electrochemical signals collected in the presence of complementary and non-complementary sequences confirmed that successful detection could be achieved in the presence of this matrix. Importantly, the neutralized sensors were stable in serum, and changes in the electrochemical current were not observed with serum alone.

The specificity of the assay was further investigated by measuring changes in the electrochemical current that occurred in the presence of targets containing one and two mismatched bases. Relative to the fully complementary target, much smaller changes in current were observed and were correlated with the number of mismatches (Supplementary Fig. S10). Further gains in specificity, if needed, could be achieved by tuning the sequence and charge of the neutralizer.

Detection of RNA. We also challenged the NDA with samples that are more heterogeneous and evaluated the assay with *Escherichia coli* total RNA. The DNA probe was designed for the RNA polymerase β-mRNA (*rpoB*), a transcript that is highly expressed in bacteria and is not conserved between species, which makes it an ideal target for bacterial detection and identification[33]. Figure 3d shows the concentration dependence of *E. coli* total RNA. 10 pg μl^{-1} *E. coli* total RNA was detected successfully, which indicates that NDA can achieve high levels of sensitivity with an excess of non-complementary material.

Detection of bacteria in unpurified lysates. The neutralizer assay was also tested with unpurified bacterial lysates. Bacterial lysates were generated by inserting solutions into a lysis chamber[34] into which strong electrical fields were introduced. This lysate was then used without further purification. Figure 3e shows the dependence of the NDA signal for differing concentrations of *E. coli* lysates. ΔI% increased with increasing concentration of *E. coli* bacteria. The horizontal dashed line represents the average ΔI% for 150 colony forming units (c.f.u.) per microlitre of non-complementary target *Staphylococcus saprophyticus*. The detection limit for *E. coli* bacteria is 0.15 c.f.u. μl^{-1}, a detection limit not achieved previously with a direct analysis that is clinically relevant for the detection of bacteria found in clinical samples. The presence of bacteria was detected successfully with high sensitivity and specificity, from sample to answer within 30 minutes.

In the trials described above, the target is complementary for the probe. We envisioned a different strategy whereby the neutralizer was specific for a target and applied this to detect a 20-mer synthetic complementary target. Here, signal post-neutralizer hybridization was increased by the removal of the two-base mismatched neutralizer from the probe and hybridization with the perfectly matched target in solution. This also led to electrocatalytic current restoration. We found that this scheme was also able to detect DNA with high specificity (see Supplementary Fig. S4).

Detection of proteins. To complete the demonstration that the NDA is universally applicable to all of the major analyte classes, we investigated whether it could detect protein biomarkers, with thrombin as a model system. The thrombin aptamer is a well-characterized sequence that is known to fold into a G-quartet structure and bind thrombin at exosite I. Figure 4a represents the protein-detection method using the neutralizer approach. A thiolated thrombin-binding aptamer was deposited onto 100 μm sensors. When neutralizers were complexed with the aptamer probes, the catalytic current was low. The current was restored in the presence of thrombin, as binding of the thrombin to the aptamer triggered neutralizer dissociation.

The electrocatalytic current was clearly suppressed on neutralizer binding to the thrombin aptamer, as exhibited in Fig. 4b. When treated with 100 pM of thrombin, a large increase in catalytic current was observed (Fig. 4b). Conversely, when treated with 100 nM of bovine serum albumin (BSA), a nonspecific protein, the signal change was negligible, which indicates that the assay was very specific for thrombin (Fig. 4c). Evaluation of ΔI% with different thrombin concentrations showed that as low as 10 fM thrombin was clearly detectable (Fig. 4d).

Multiplexing capabilities. The flexibility of the neutralizer assay, coupled with the use of a chip with multiple sensors, allows for the analysis of multiple analytes. For example, cocaine and ATP could be monitored simultaneously using sensors modified with each aptamer. As shown in Supplementary Fig. S8, even

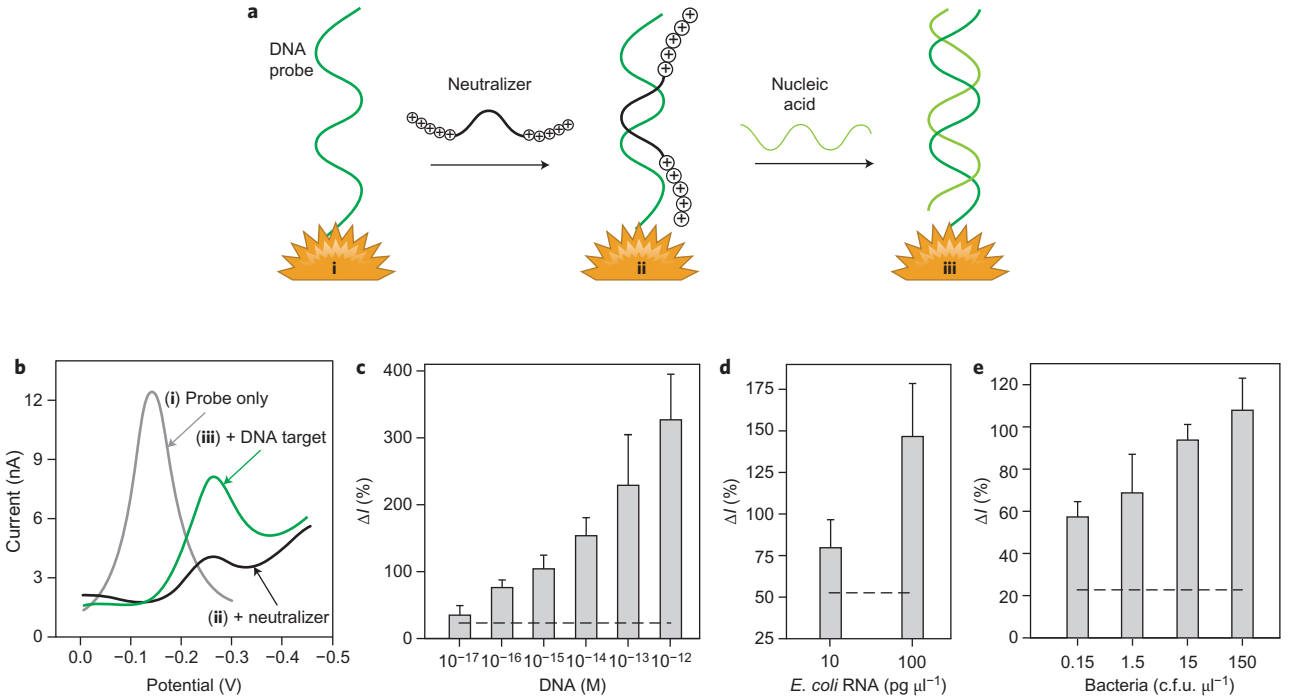

Figure 3 | NDA nucleic acid and bacterial detection. a, Schematic representation of NDA nucleic acid detection strategy. **b**, DPV signals for a DNA probe-modified sensor (**i**), after neutralizer binding to the probe (**ii**) and after treatment with 1 pM of 20-mer synthetic target DNA (**iii**). **c**, Concentration-dependent signal change for a 20-mer synthetic DNA target. The horizontal dashed line indicates the average signal change in the presence of a 100 nM non-complementary 20-mer target. **d**, Concentration-dependent signal change for *E. coli* total RNA. The horizontal dashed line indicates the average signal change in the absence of the target; the probe used was complementary to *rpoB*. **e**, Concentration-dependent signals observed with *E. coli* lysates. The horizontal dashed line indicates the average signal change in the presence of 150 c.f.u. μl^{-1} *S. saprophyticus* lysate. Error bars represent the standard error and are collected from at least three independent experiments on three chips that have 20 sensors. Averaged data from single chips exhibit significantly lower error values (<20%).

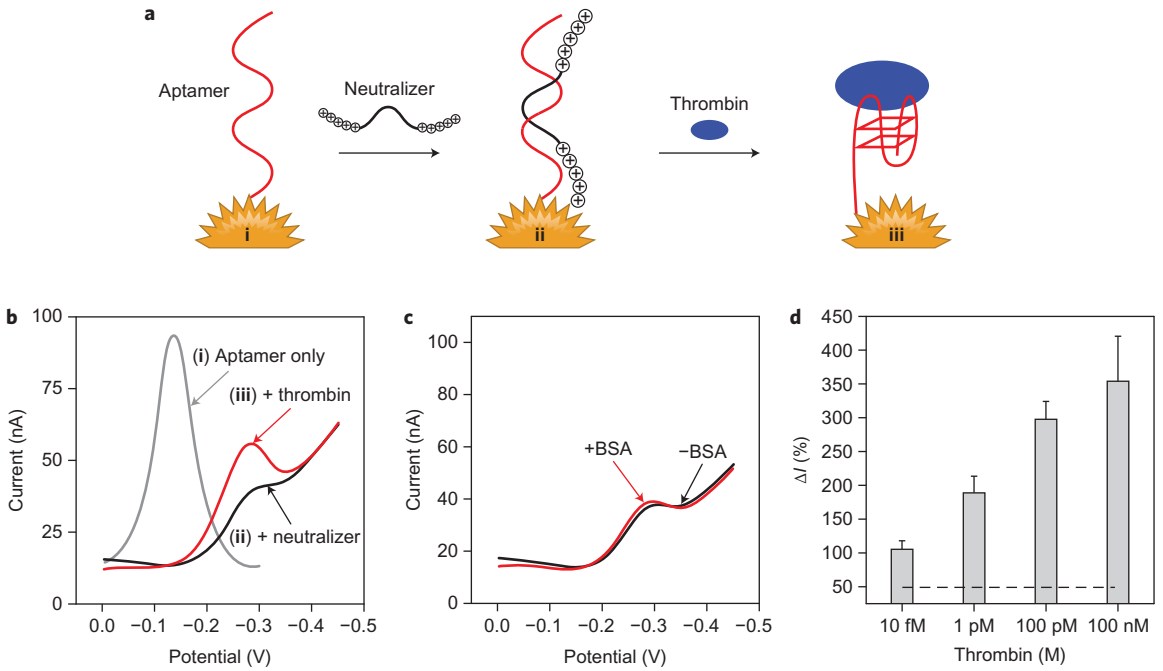

Figure 4 | NDA protein detection. a, Schematic representation of NDA thrombin detection. **b**, DPV signals for thrombin-binding aptamer-modified sensor (**i**), after neutralizer binding to the aptamer (**ii**) and after treatment with 100 pM thrombin (**iii**). **c**, DPV signals before (black line) and after (red line) the addition of 100 nM BSA. **d**, Concentration-dependent signals for NDA thrombin detection. The horizontal dashed line indicates the average signal change in the presence of 100 nM BSA, a nonspecific protein. Error bars represent the standard error and are collected from at least three independent experiments on three chips that have 20 sensors. Averaged data from single chips exhibit significantly lower error values (<20%).

when mixtures of the two molecules were analysed at concentrations that correspond to the limits of detection for the assay, successful detection was achieved with an acceptable level of specificity.

The extent of multiplexing that could be achieved with this approach is governed only by the chip design. To functionalize individual sensors with specific aptamers or probes, sufficient spacing between sensors, or barriers between sensors, must be introduced. With the lithographic techniques used to fabricate the chip design employed in this study, multiplexing of 100 different analytes could probably be achieved as long as sufficient sensor separation could be achieved.

Only a few examples in the literature exhibit the detection of molecularly diverse analytes. Xia et al. developed, using Au nanoparticles and conjugated polyelectrolytes, a colorimetric sensor to detect DNA, small molecules, proteins and ions[1]. However, the sensitivity towards nucleic acid analytes was not sufficient for use without enzymatic amplification. The universal detection system presented here is the first to achieve sensitivity with all of the major classes of analytes. Moreover, the concept that underlies the NDA is applicable to all sensing platforms where charge changes are relevant, including FETs and cantilevers. The development of this approach should spur further advances in the detection of small-molecule analytes using simple instrumentation.

Materials and methods

Materials. Adenosine 5′-triphosphate disodium salt, human thrombin, BSA, $HAuCl_4$ solution, potassium ferrocyanide trihydrate ($K_2[Fe(CN)_6{\cdot}3H_2O$), hexammine ruthenium(III) chloride ($Ru(NH_3)_6Cl_3$), $MgCl_2$, 10× tris-borate-EDTA buffer, Ultrapure Agarose, dimethyl formamide, piperidine, trifluoroacetic acid, *m*-cresol, triisopropylsilane, diethyl ether and dithiothreitol (DTT) were obtained from Sigma-Aldrich. ACS-grade acetone, isopropyl alcohol and perchloric acid were obtained from EMD; 6N hydrochloric acid was purchased from VWR. Phosphate-buffered saline (PBS, pH 7.4, 1×) and SYBR Au gel staining dye were obtained from Invitrogen. 6× DNA loading dye and a 100 base pair DNA ladder were obtained from Fermentas. Cocaine was obtained from Cerillian (Round Rock, Texas) and *E. coli* total RNA from Ambion, Inc. The ATP-binding aptamer, cocaine-binding aptamer and thrombin-binding aptamer were obtained from Integrated DNA Technologies (Coralville, Indiana). PNA monomers were obtained from Link Technologies (Lanarkshire, Scotland), Fmoc-Lys(Boc)-OH from Advanced ChemTech (Louisville, Kentucky), Knorr resin from NovaBioChem and HATU (*O*-(7-azabenzotriazol-1-yl)-*N*,*N*,*N*′,*N*′-tetramethyluronium hexafluorophosphate) from Protein Technologies Inc. (Tucson, Arizona).

The *E. coli* DNA probe used to detect the synthetic 20-mer target DNA, *E. coli* total RNA and *E. coli* lysate was obtained from the Centre for Applied Genomics in the Hospital for Sick Children (Toronto, Canada). A thiol-containing linker was added on the 5′-terminus in-house as in our previously published work[35]. 20-mer complementary and non-complementary target DNA sequences were obtained from the ACGT Corporation (Toronto, Canada).

Neutralizers were synthesized using a solid-phase synthesis approach on a Prelude automated peptide synthesizer (Protein Technologies, Inc.). All synthesis products were confirmed by mass spectroscopy.

All probe molecules and neutralizers were purified stringently using an Agilent 1100 Series HPLC. Concentration was quantified by measuring absorbance at 260 nm.

Chip fabrication. Chips were fabricated at Advanced Micro Systems (Ottawa, Canada). Silicon wafers (six inches (15.24 cm)) were passivated using a thick layer of thermally grown silicon dioxide. A 25 nm Ti layer was deposited on the silicon dioxide. A 350 nm Au layer was deposited on the chip using electron beam assisted Au evaporation. The Au film was patterned using a standard photolithography and lift-off process. A 5 nm Ti layer was deposited on the Au film. A 500 nm layer of insulating Si_3N_4 was deposited using chemical vapour deposition; 5 μm apertures were imprinted on the electrodes using standard photolithography and 0.4 mm × 2 mm bond pads were exposed using standard photolithography.

Fabrication of NMEs. Chips were cleaned by sonication in acetone for five minutes, rinsed with isopropyl alcohol and deionized water for 30 seconds and dried with a flow of nitrogen. Electrodeposition was performed at room temperature; 5 μm apertures on the fabricated electrodes were used as the working electrode and were contacted using the exposed bond pads. Au sensors were made using a deposition solution containing a 50 mM solution of $HAuCl_4$ and 0.5 M HCl. The 100 μm and 20 μm Au structures were formed using direct current potential amperometry at 0 mV for 100 seconds and 0 mV for 20 seconds, respectively. After washing with deionized water and drying, the Au sensors were coated with Pd to form nanostructures by replating in a solution of 5 mM H_2PdCl_4 and 0.5 M $HClO_4$ at −250 mV for ten seconds (for the 100 μm structure) and for five seconds (for the 20 μm structure).

NDA protocol. All thiolated aptamers and thiolated DNA probes were deprotected using DTT followed by purification with high-performance liquid chromatography (HPLC) and the HPLC-purified probes were lyophilized and stored at −20 °C. For immobilization of the probe, phosphate buffer solution (25 mM, pH 7) containing 5 μM thiolated probe, 25 mM NaCl and 50 mM $MgCl_2$ was incubated with the sensors for one hour in a dark humidity chamber at room temperature. Then the chip was washed twice for five minute with phosphate buffer solution (25 mM) containing 25 mM NaCl. Next, sensors were incubated for 30 minutes at room temperature with a phosphate buffer solution (25 mM) containing 10 μM neutralizer and 25 mM NaCl, followed by washing three times for five minutes each with the same buffer. Subsequently, chips were treated with different targets followed by washing. For ATP detection, sensors were incubated for ten minutes at room temperature with a phosphate buffer solution (25 mM) containing 25 mM NaCl and different concentrations of ATP. For cocaine detection, sensors were incubated for two minutes at room temperature with a phosphate buffer solution (25 mM) containing 25 mM NaCl and different concentrations of cocaine. For synthetic target DNA, sensors were incubated for 30 minutes at room temperature with a phosphate buffer solution (25 mM) containing 25 mM NaCl, 10 mM $MgCl_2$ and different concentrations of the target. In the cases of *E. coli* total RNA and *E. coli* lysate, sensors were incubated for 30 minutes at room temperature with sterile and RNase-free PBS containing different concentrations of the target.

Electrochemical analysis and scanning electron microscopy (SEM). All electrochemical experiments were carried out using a Bioanalytical Systems Epsilon potentiostat with a three-electrode system featuring a Ag/AgCl reference electrode and a platinum wire auxiliary electrode. Electrochemical signals were measured in a 25 mM phosphate buffer solution (pH 7) containing 25 mM NaCl, 10 μM $[Ru(NH_3)_6]Cl_3$ and 4 mM $K_3[Fe(CN)_6]$. DPV signals were obtained with a potential step of 5 mV, pulse amplitude of 50 mV, pulse width of 50 ms and a pulse period of 100 ms. Signal changes that corresponded to replacement of the neutralizer by a specific target were calculated with background-subtracted currents: $\Delta I\% = (I_{after} - I_{before})/I_{before} \times 100$ (where I_{after} = current after replacement of neutralizer and I_{before} = current before replacement of neutralizer). SEM images were obtained using an Aspex 3025 SEM.

Received 6 February 2012; accepted 24 April 2012; published online 3 June 2012

References

1. Xia, F. *et al.* Colorimetric detection of DNA, small molecules, proteins, and ions using unmodified gold nanoparticles and conjugated polyelectrolytes. *Proc. Natl Acad. Sci. USA* **107,** 10837–10841 (2010).
2. Zhang, M., Win, B. C., Tan, W. & We, B. C. A versatile graphene-based fluorescence 'on/off' switch for multiplex detection of various targets. *Biosens. Bioelectron.* **26,** 3260–3265 (2011).
3. Drummond, T. G., Hill, M. G. & Barton, J. K. Electrochemical DNA sensors. *Nature Biotechnol.* **21,** 1192–1199 (2008).
4. Clack, N. G., Asalaita, K. & Groves, J. T. Electrostatic readout of DNA microarrays with charged microspheres. *Nature Biotechnol.* **26,** 825–830 (2008).
5. Morrow, T. J., Li, M., Kim, J., Mayer, T. S. & Keating, C. D. Programmed assembly of DNA-coated nanowire devices. *Science* **323,** 352 (2009).
6. Zheng, G., Patolsky, F., Cui, Y., Wang, U. W. & Lieber, C. M. Multiplexed electrical detection of cancer markers with nanowire sensors arrays. *Nature Biotechnol.* **23,** 1294–1300 (2005).
7. Patolsky, F., Zheng, G. & Lieber, C. M. Fabrication of silicon nanowire devices for ultrasensitive, label-free, real-time detection of biological and chemical species. *Nature Protocols* **1,** 1711–1724 (2006).
8. Tian, B. *et al.* Three-dimensional, flexible nanoscale field-effect transistors as localized bioprobes. *Science* **13,** 830–834 (2010).
9. Zheng. G., Gao, X. P. A. & Lieber, C. M. Frequency domain detection of biomolecules using silicon nanowire biosensors. *Nano Lett.* **10,** 3179–3183 (2010).
10. Wu, G *et al.* Bioassay of prostate-specific antigen (PSA) using microcantilevers. *Nature Biotechnol.* **19,** 856–860 (2001).
11. Fritz, J. *et al.* Translating biomolecular recognition into nanomechanics. *Science* **288,** 316–318 (2000).
12. Xiang, Y. & Lu, Y. Using personal glucose meters and functional DNA sensors to quantify a variety of analytical targets. *Nature Chem.* **3,** 697–670 (2011).
13. Cheng, A. K. H., Ge, B. X. & Yu, H. Z. Label-free voltammetric detection of lysozyme with aptamer-modified gold electrodes. *Anal. Chem.* **79,** 5158–5164 (2007).
14. Baker, B. R. *et al.* An electronic, aptamer-based small molecule sensor for the rapid, reagentless detection of cocaine in adulterated samples and biological fluids. *J. Am. Chem. Soc.* **128,** 3138–3139 (2006).

15. Xiao, Y., Lai, R. Y. & Plaxco, K. W. Preparation of electrode-immobilized, redox-modified oligonucleotides for electrochemical DNA and aptamer-based sensing. *Nature Protocols* **2,** 2875–2880 (2007).
16. Cash, K. J., Ricci, F. & Plaxco, K. W. An electrochemical sensor for the detection of protein–small molecule interactions directly in serum and other complex matrices. *J. Am. Chem. Soc.* **131,** 6955–6957 (2009).
17. Zuo, X. *et al.* A target-responsive electrochemical aptamer switch (TREAS) for reagentless detection of nanomolar ATP. *J. Am. Chem. Soc.* **129,** 1042–1043 (2007).
18. Das, J., Aziz, M. A. & Yang, H. A nanocatalyst-based assay for proteins: DNA-free ultrasensitive electrochemical detection using catalytic reduction of *p*-nitrophenol by gold-nanoparticle labels. *J. Am. Chem. Soc.* **128,** 16022–16023 (2006).
19. Das, J., Jo, K., Lee, J. W. & Yang, H. Electrochemical immunosensor using *p*-aminophenol redox cycling by hydrazine combined with a low background current. *Anal. Chem.* **79,** 2790–2796 (2007).
20. Das, J., Lee, J-A. & Yang, H. Ultrasensitive detection of DNA in diluted serum using $NaBH_4$ electrooxidation mediated by $[Ru(NH_3)_6)]^{3+}$ at indium–tin oxide electrodes. *Langmuir* **26,** 6804–6808 (2010).
21. Xiang, Y., Xie, M., Bash, R., Chen, J. J. L. & Wang, J. Ultrasensitive label-free aptamer-based electronic detection. *Angew. Chem. Int. Ed.* **119,** 9212–9214 (2007).
22. Plaxco, K. W. & Soh, H. T. Switch-based biosensors: a new approach towards real-time, in vivo molecular detection. *Trends Biotechnol.* **29,** 1–5 (2011).
23. Lai, R. L. *et al.* Rapid, sequence-specific detection of unpurified PCR amplicons via a reusable, electrochemical sensor. *Proc. Natl Acad. Sci. USA* **103,** 4017–4021 (2006).
24. Lapierre, M. A., O'Keefe, M. M., Taft, B. J. & Kelley, S. O. Electrocatalytic detection of pathogenic DNA sequences and antibiotic resistance markers. *Anal. Chem.* **75,** 6327–6333 (2003).
25. Soleymani, L., Fang, Z., Sargent, E. H. & Kelley, S. O. Programming the detection limits of biosensors through controlled nanostructuring. *Nature Nanotechnol.* **4,** 844–848 (2009).
26. Soleymani, L. *et al.* Nanostructuring of patterned microelectrodes to enhance the sensitivity of electrochemical nucleic acids detection. *Angew. Chem. Int. Ed.* **48,** 8457–8460 (2009).
27. Yang, H. *et al.* Direct, electronic microRNA detection reveals differential expression profiles in 30 minutes. *Angew. Chem. Int. Ed.* **48,** 8461–8464 (2009).
28. Fang, Z. *et al.* Direct profiling of cancer biomarkers in tumour tissue using a multiplexed nanostructured microelectrode integrated circuit. *ACS Nano* **3,** 3207–3213 (2009).
29. Das, J. & Kelley, S. O. Protein detection using arrayed microsensor chips: tuning sensor footprint to achieve ultrasensitive readout of CA-125 in serum and whole blood. *Anal. Chem.* **83,** 1167–1172 (2011).
30. Soleymani, L. *et al.* Hierarchical nanotextured microelectrodes overcome the molecular transport barrier to achieve rapid, direct bacterial detection. *ACS Nano* **5,** 3360–3366 (2011).
31. Vasilyeva, E., Fang, Z., Minden, M., Sargent, E. H. & Kelley, S. O. Direct genetic analysis of ten cancer cells: tuning molecular probe design for efficient mRNA capture *Angew. Chem. Int. Ed.* **50,** 4137–4141 (2011).
32. Su, L., Sankar, C. G., Sen, D. & Yu, H-Z. Kinetics of ion-exchange binding of redox metal cations to thiolate–DNA monolayers on gold. *Anal. Chem.* **76,** 5953–5959 (2004).
33. Bernstein, J. A., Khodursky, A. B., Lin, P. H., Lin-Chao, S. & Cohen, S. N. Global analysis of mRNA decay and abundance in *Escherichia coli* at single-gene resolution using two-color fluorescent DNA microarrays *Proc. Natl Acad. Sci. USA* **99,** 9697–9702 (2002).
34. Lam, B., Fang, Z., Sargent, E. H. & Kelley, S. O. Polymerase chain reaction-free, sample-to-answer bacterial detection in 30 minutes with integrated cell lysis. *Anal. Chem.* **84,** 21–25 (2012).
35. Taft, B. J., O'Keefe, M., Fourkas, J. T. & Kelley, S. O. Engineering DNA-electrode connectivities: manipulation of linker length and structure. *Anal. Chim. Acta* **496,** 81–91 (2003).

Acknowledgements

We acknowledge the Natural Sciences and Engineering Research Council (Discovery Grant to S.O.K.), Mitacs (Elevate Fellowship to J.D.) and the Defense Advanced Research Projects Agency (DXoD programme funding to S.O.K. and E.H.S.) for their support of this work.

Author contributions

S.O.K. and J.D. conceived the experiments. J.D., K.B.C., A.Z. and P.L. performed the experiments. J.D., K.B.C., A.Z., P.L., E.H.S. and S.O.K. discussed the results. J.D., K.B.C., E.H.S. and S.O.K. co-wrote and edited the manuscript.

Additional information

The authors declare no competing financial interests. Supplementary information accompanies this paper at www.nature.com/naturechemistry. Reprints and permission information is available online at http://www.nature.com/reprints. Correspondence and requests for materials should be addressed to S.O.K.